atmosphere

MDPI

Article

Speciation of Magnesium in Aerosols Using X-ray Absorption Near-Edge Structure Related to Its Contribution to Neutralization Reactions in the Atmosphere

Takahiro Kawai [1], Yoshiaki Yamakawa [1] and Yoshio Takahashi [1,2,*]

[1] Department of Earth and Planetary Science, Graduate School of Science, The University of Tokyo, Hongo 7-3-1, Bunkyo, Tokyo 113-0033, Japan; taka_k@eps.s.u-tokyo.ac.jp (T.K.); yotiotakaha@yahoo.co.jp (Y.Y.)

[2] Photon Factory, Institute of Materials Structure Science, High Energy Accelerator Research Organization (KEK), Tsukuba, Ibaraki 305-0801, Japan

* Correspondence: ytakaha@eps.s.u-tokyo.ac.jp; Tel.: +81-3-5841-4517

Abstract: Aerosols, including mineral dust, are transported from China and Mongolia to Japan, particularly in spring. It has been recognized that calcium (Ca) carbonate is the main Ca species in aerosols, which reacts with acidic species such as sulfuric and nitric acids at the surface of mineral dust during its long-range transport, related to mitigation of acid depositions. The similar assumption that magnesium (Mg) originally takes the form of carbonate and contributes to the neutralization reaction and buffering effect on the acidity of aerosols has been suggested in various studies. However, few studies have confirmed this process by measuring actual Mg species in aerosols quantitatively. In this study, X-ray absorption near-edge structure (XANES) spectroscopy was employed to determine Mg species in size-fractionated aerosol samples, including mineral dust. The results showed that (i) most Mg in the mineral dust did not take the form of carbonate and its reacted species (e.g., sulfate and nitrate) produced by the neutralization reaction, but (ii) Mg was mainly found as Mg in the octahedral layer in phyllosilicates. Given that the reactivity of such Mg in phyllosilicates is much lower than those in carbonate minerals, the contribution of Mg to the neutralization reactions in the atmosphere must be lower than previously expected.

Keywords: aerosol; mineral dust; speciation; XANES; neutralization reaction

Citation: Kawai, T.; Yamakawa, Y.; Takahashi, Y. Speciation of Magnesium in Aerosols Using X-ray Absorption Near-Edge Structure Related to Its Contribution to Neutralization Reactions in the Atmosphere. *Atmosphere* **2021**, *12*, 586. https://doi.org/10.3390/atmos12050586

Academic Editor: Anthony Joseph Hynes

Received: 8 April 2021
Accepted: 29 April 2021
Published: 1 May 2021

1. Introduction

Calcium carbonate is the most common Ca species in aerosols or mineral dust (coarse particle-size fraction in aerosols usually over 1 μm) [1,2]. This mineral is an important component in aerosols because it is reactive with acidic species such as sulfuric acid, nitric acid, and organic acids in the atmosphere [3–5]. As a result, Ca in aerosols can mitigate acid deposition through the neutralization of acidic species, which produces Ca nitrate, Ca sulfate, and Ca oxalate in aerosols [2,6,7]. Meanwhile, many studies have assumed that most Mg in the atmosphere is present as Mg carbonate (e.g., dolomite and magnesite) in aerosols [5,8], which can also react with acidic species. The amount of Mg species in aerosol have been indirectly estimated using the charge balances of soluble cations and anions and the water solubilities of various salts [5]. From another aspect, carbonate minerals can be buffers to control the acidity of aerosols, which in turn regulates the solubility of Fe, an important component in aerosols related to ocean productivity [9,10]. In such studies, the presence of Mg carbonate has been also assumed (e.g., Myriokefalitakis et al. [11]).

However, Mg can also form primary minerals (e.g., silicates) and phyllosilicates (e.g., clay minerals such as montmorillonite and chlorite [12]), the latter of which can be a main component of mineral dust because of their high abundance at earth's surface and small particle sizes [13–15]. However, to the best of our knowledge, quantitative determination of various Mg species in aerosols has yet to be conducted.

In the present study, we employed X-ray absorption near-edge structure (XANES) at Mg K-edge for the speciation of Mg in aerosols. XANES spectroscopy has been used for the speciation of various elements in aerosols such as Ca, sulfur (S), iron (Fe), and lead (Pb) [1,2,16–18], suggesting that the method is a useful tool for the speciation of various elements in aerosols, especially because the amount of aerosol samples recovered is generally lower than that needed for X-ray diffraction. However, XANES studies for the speciation of Mg in aerosols remain lacking because the X-ray energy at Mg K-edge (=1.303 keV) is located in the soft X-ray energy region, where XANES is less frequently applied compared with those in the hard X-ray region. Thus, this study employs Mg K-edge XANES as a direct speciation method for Mg in aerosols, and the result will be compared with those obtained for Ca in the same aerosol samples.

2. Materials and Methods

Aerosol samples employed in this study were collected on a cellulose aerosol filter (TE-230WH, Tisch Environmental Inc., OH, USA) by using a high-volume air sampler (Kimoto, MODEL-123SL, Osaka, Japan) with a cascade impactor (Series 230, Tisch Environmental Inc.) on the roof of a building in Higashi–Hiroshima City (latitude, 34.40° N; longitude, 132.71° E; height, approximately 10 m above the ground) from 8 to 20 April, 2012. Backward trajectory analysis was performed using the hybrid single-particle Lagrangian-integrated trajectory (HYSPLIT) model to identify the source of each sample [19]. The aerosols were separated into seven size fractions using the cascade impactor (Stage 1, >10.2 μm; Stage 2, 4.2–10.2 μm; Stage 3, 2.1–4.2 μm; Stage 4, 1.3–2.1 μm; Stage 5, 0.69–1.3 μm; Stage 6, 0.39–0.69 μm; Stage 7 backup filter [BF], <0.39 μm). Details of the samples were described in our previous studies [7,20].

Chemical analysis was conducted for total and water-soluble fractions of various elements. Water-soluble major ions (Na^+, NH_4^+, K^+, Mg^{2+}, Ca^{2+}, Cl^-, NO_3^-, and SO_4^{2-}) were analyzed using ion chromatography. Approximately 40 mg of the filter was soaked in 5 mL of Milli-Q water with ultrasonic treatment for 30 min. Each sample solution was filtered through a 0.20 μm PTFE filter (DISMIC-25HP, ADVANTEC, Tokyo, Japan) and analyzed by ion chromatography (IC7000, Yokogawa, Tokyo, Japan). Shima-pack IC-SA1/-SA1(G) columns were used, and the eluent composition was 14 mM $NaHCO_3$ at a flow rate of 1.0 mL/min. Acid digestion was also conducted to investigate the total concentrations of aluminum (Al), Mg, Ca, zinc (Zn), and Pb by inductively coupled plasma–atomic emission spectroscopy (ICP-AES; SII Nano Technology, Inc., SP3500, Chiba, Japan) or inductively coupled plasma–mass spectrometry (Agilent 7700, Tokyo, Japan). Total decomposition of the samples was conducted by mixed acid digestions as reported in the study by Kurisu et al. [20].

XANES spectra at Mg K-edge were obtained at BL-10 of the Synchrotron Radiation Center, Ritsumeikan University (Shiga, Japan). Some of the spectra were also obtained at BL27XU in SPring-8 (Hyogo, Japan), which showed the spectra identical to those recorded at Ritsumeikan University. In BL-10, incident X-ray at a certain energy was obtained using a double-crystal monochromator of Beryl (10-10). X-ray energy was calibrated by defining the XANES peak of MgO as 1309.27 eV. XANES spectra for reference materials were recorded in total electron yield mode, whereas those for the aerosol samples were in fluorescence mode, using a silicon drift detector. A small piece of the cellulose filter (size: ca. 3×3 mm^2) with aerosol samples was loaded on an aluminum sample holder, which was exposed to the incident beam that had a similar size to the sample. For comparison, Ca speciation was also conducted by Ca K-edge XANES measured at BL-9A at the Photon Factory (Tsukuba, Japan). Details of the Ca K-edge XANES were identical to those reported in our previous studies [1,7]. Linear combination fitting (LCF) of each spectrum by endmembers of possible Mg or Ca species and principal component analysis (PCA) to obtain the number of endmembers needed for the LCF were conducted using Athena software [21]. The number of parameters needed to explain all the spectra of Mg and Ca spectra estimated by PCA were 4 and 5, respectively.

3. Results

3.1. Concentrations of Various Elements in the Aerosol Samples

The results of the 72 h backward trajectory analysis by HYSPLIT (Figure 1) suggested that the samples collected in Higashi–Hiroshima employed in this study were transported from northeast China and Mongolia to Japan, generally observed in spring in East Asia [2,4]. Concentrations of major elements, Zn and Pb, in the atmosphere, are shown in Figure 2. Among them, the concentration of Ca in the coarse fractions (>1.7 μm; mineral dust), often regarded as a tracer of crustal materials, was higher (ca. 20 nmol/m^3 in each fraction) compared with those in our observations in other seasons in 2012 (<5 nmol/m^3 reported in Miyamoto et al. [7]). This result supported that the mineral dust was transported from the continent to Japan. The size distribution of Mg shows that most of the Mg was found in fractions larger than 1.7 μm, which is similar to that of Ca, suggesting that Mg is also of crustal origin. For Mg, however, the contribution of sea salt particles cannot be ignored. Thus, concentration of non-sea-salt Mg in the atmosphere (=[nss-Mg]) was determined based on the equation below:

$$[\text{nss-Mg}] = [\text{Mg}] - [\text{ss-Na}] \times \alpha_{\text{Mg}}$$

where α_{Mg} is the Mg to Na molar ratio in bulk seawater [22]. Since crustal Na contribution relative to sea-salt Na cannot be ignored in particular in the dust period, sea-salt Na concentration (= [ss-Na]) in this study was determined as shown below:

$$[\text{ss-Na}] = [\text{Na}] - [\text{Al}] \times \beta_{\text{Na}}$$

where β_{Na} was the Na to Al molar ratio in the average crust [23]. The [nss-Mg] was plotted in Figure 2b, showing that more than 63% of total Mg was of crustal origin (Figure 2d), which could be confirmed by enrichment factor (EF).

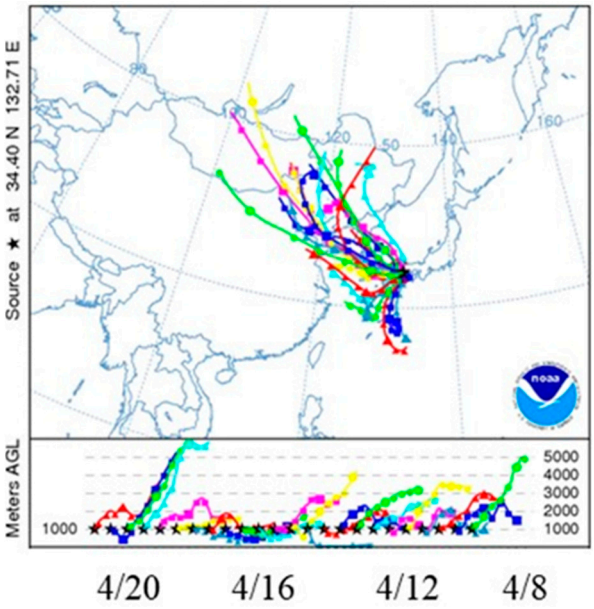

Figure 1. Backward trajectories during the sampling period (8 to 20 April, 2012) in Higashi-Hiroshima. The trajectories started at the height of 1000 m above the sampling site in Higashi-Hiroshima, and run time was 72 h.

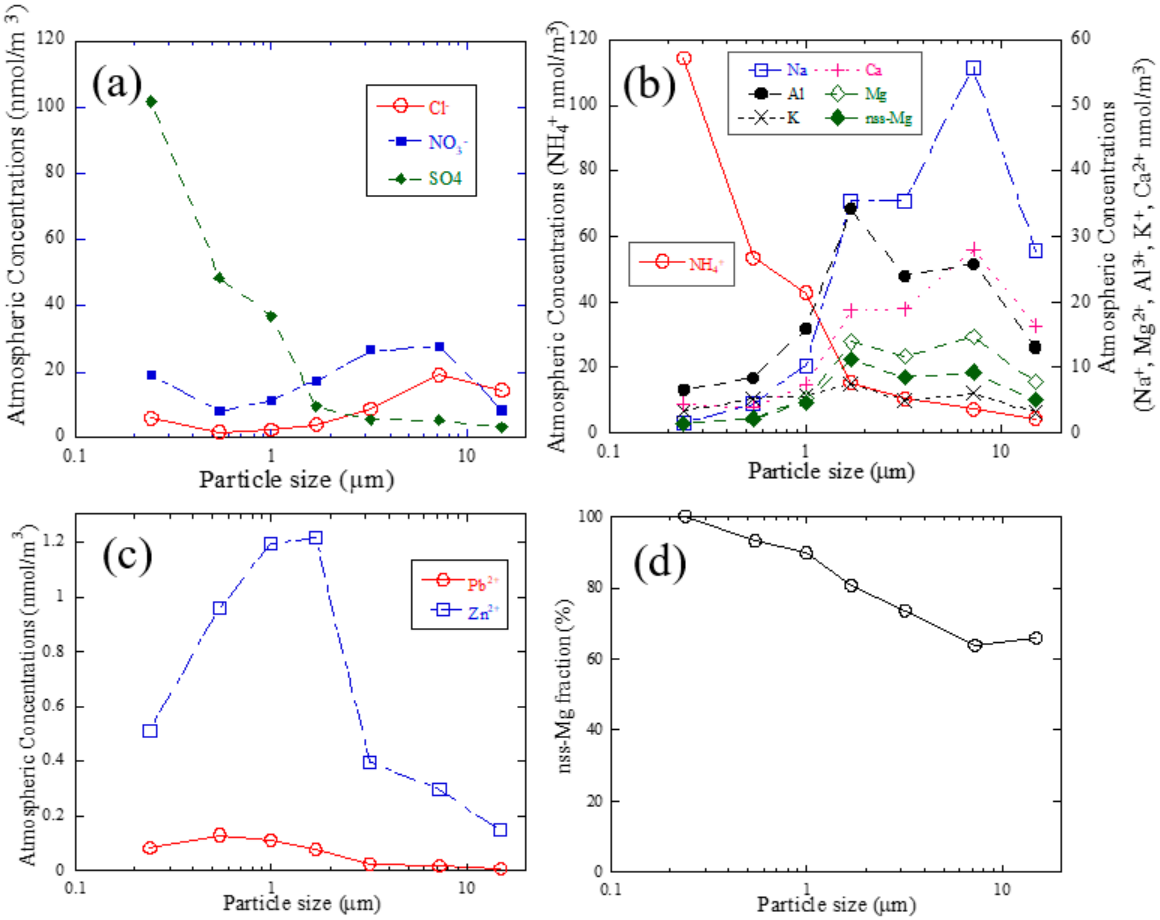

Figure 2. Atmospheric concentrations of (**a**) major anions (water extraction), (**b**) major cations (acid digestion), (**c**) trace elements (Zn and Pb; acid digestion), and (**d**) the ratio of nss-Mg to total Mg.

Ratios of total concentrations of Ca, Mg (nss-Mg), Zn, and Pb relative to Al determined by acid digestion were normalized to those of crustal materials to obtain EF (Figure 3). The EF here was defined for an element M, EF(M), as follows:

$$EF(M) = ([M]_{sample}/[Al]_{sample})/([M]_{crust}/[Al]_{crust}) \quad (1)$$

where [] values denote their molar concentrations. The average concentration in crustal materials, $[X]_{crust}$, for the element X, is referred to by Taylor and McLennan [23]. In general, an EF(M) larger than 10 suggests that M originated from anthropogenic sources, whereas an EF(M) ranging from 1 to 10 suggests that M originated from natural sources [7,24]. The EF(Ca) and EF(Mg) were close to unity at any particle sizes (Figure 3), but the EF(Zn) values were above 10 and 100 in the coarse (>1 μm) and fine (<1 μm) particle sizes, respectively, reflecting the dominance of anthropogenic sources of Zn contained in the samples. The EF(Pb) results exhibited a similar trend to that of Zn. These results showed that Ca and Mg were of natural origins, whereas Zn and Pb mainly of anthropogenic.

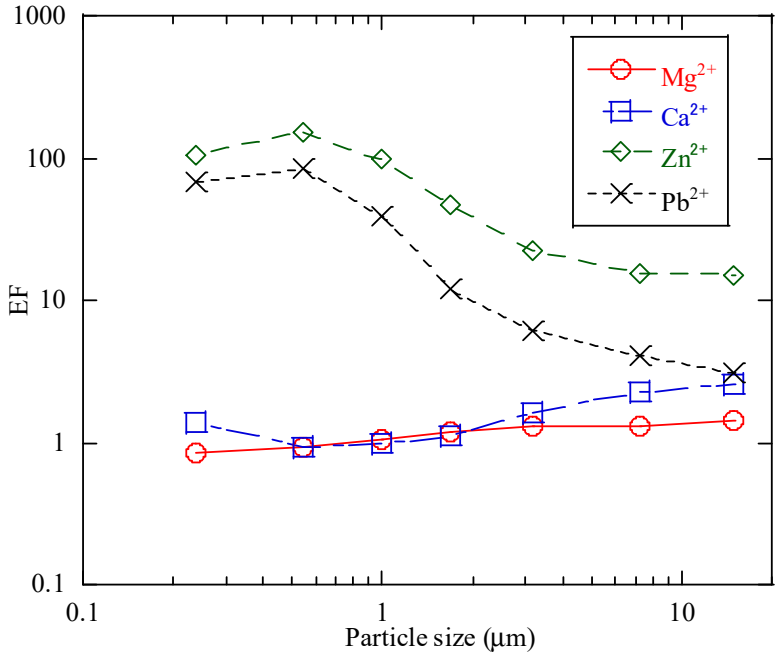

Figure 3. Enrichment factor (EF) relative to crustal abundances for Mg (nss-Mg), Ca, Zn, and Pb in the aerosol samples.

3.2. Speciation of Ca by Ca K-Edge XANES

Following our previous studies on aerosols collected in Japan [1,2,7], calcite, gypsum ($Ca(SO_4)\cdot 2H_2O$), Ca chloride ($CaCl_2\cdot 2H_2O$), Ca nitrate ($Ca(NO_3)_2\cdot 4H_2O$), and Ca oxalate ($CaC_2O_4\cdot 2H_2O$) were considered as possible Ca species that could be contained in aerosols for the speciation analysis using Ca K-edge XANES (Figure 4a). The spectra were similar to those reported in other seasons in Higashi–Hiroshima [7], reflecting the presence of gypsum as a main Ca species. Further quantitative analysis was conducted based on the fitting of the spectra by the model spectra obtained by the linear combination of the species above (linear combination fitting, LCF). The results showed that gypsum and calcium chloride were main Ca species at any particle sizes (Figure 5). This result is consistent with previous results for Ca species in aerosols in various sites in Japan [1,2,7,25], suggesting the validity of the present results. In the view that most Ca in aerosols are of crustal origin, initially present as calcite [1,2,7], the chloride and sulfate formed secondarily as a result of the reaction of calcite with acidic species (e.g., sulfuric acid) at mineral surfaces. Calcium chloride can also form through the dissolution of Ca from calcite by reactions with acids and then finally precipitate as chloride in the aerosols. According to previous results [1,2,7], these secondary species formed at the calcite surfaces found in the coarser particles by the neutralization reactions with acidic species. This process is supported by the fact that a relatively larger amount of calcite remains in the coarser particles (Figure 4b; circa 30% of Ca species were calcite in the 7.2 and 15 μm fractions), possibly because of the neutralization reactions occurring selectively at the particle surface.

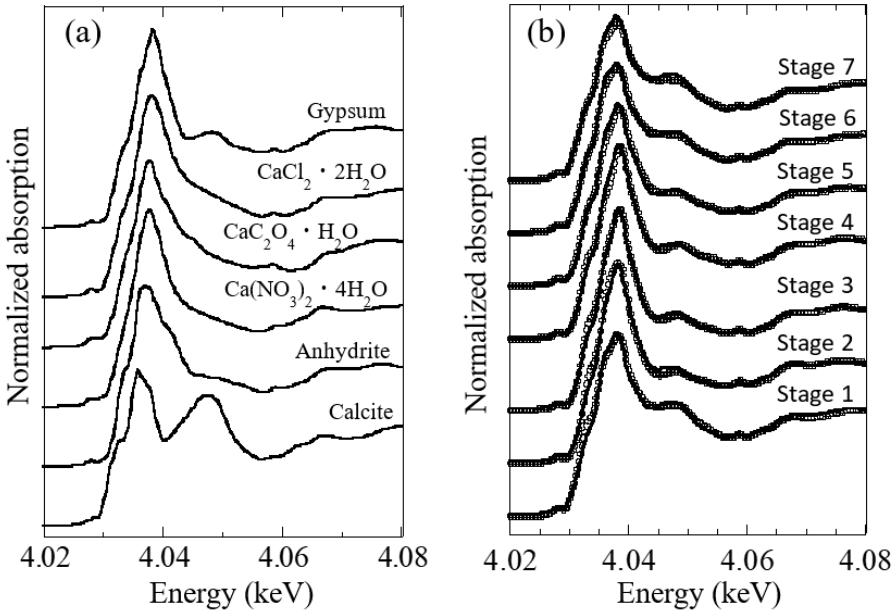

Figure 4. XANES spectra at Ca K-edge for (**a**) Ca reference materials and (**b**) Ca in size-fractionated aerosol samples. Circles and solid curves in (**b**) showed measured spectra and spectra obtained by LCF analysis, respectively.

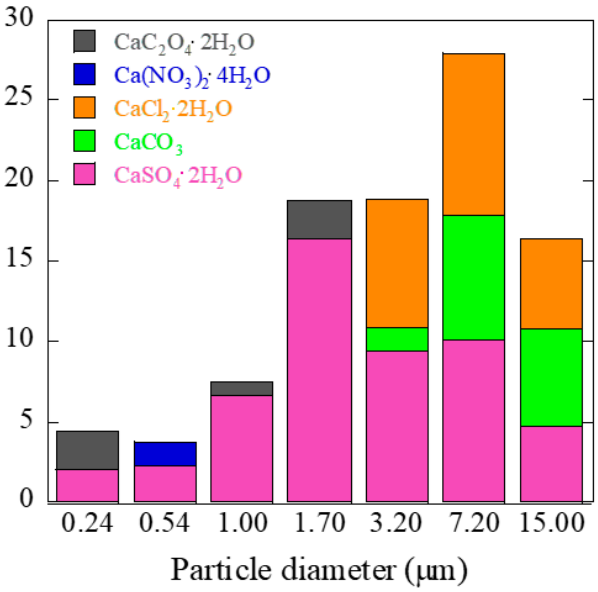

Figure 5. Speciation of Ca in aerosols determined by XANES analyses.

3.3. Speciation of Mg by Mg K-Edge XANES

The reference materials of Mg species employed for Mg K-edge XANES analysis (Figure 6) can be divided into five categories: (i) montmorillonite (one type of smectite), which represents octahedral Mg in the 2:1 phyllosilicate including illite and chlorite; the three minerals are the main Mg-bearing minerals in desert sand, the loss plateau, and dust collected in East China [15,24,26]; (ii) carbonate minerals including $MgCO_3$ (magnesite), $CaMg(CO_3)_2$ (dolomite), and $MgCO_3 \cdot Mg(OH)_2$; (iii) Mg_2SiO_4 (olivine representing octahedral silicate); (iv) MgO; and (v) Mg salts, such as $MgCl_2 \cdot 6H_2O$, $Mg(NO_3)_2 \cdot 4H_2O$, $MgC_2O_4 \cdot 2H_2O$, and $MgSO_4 \cdot 7H_2O$. The Mg in the octahedral layer in phyllosilicates showed three peculiar peaks at 1311, 1316.5, and 1316.5 eV (Figure 6a), which are clearly different from those of other species. Considering that similar spectra with three peaks were also observed for other octahedral Mg in phyllosilicates such as illite and chlorite [27,28],

we treated the montmorillonite spectrum representing Mg in these phyllosilicates. As for category (v), if we assume neutralization processes as observed for calcium [1,2,5,7,8], the category (v) species can be produced secondarily in the atmosphere by reactions with acids. Such processes can be important, especially when Mg is initially present as carbonate in the aerosols.

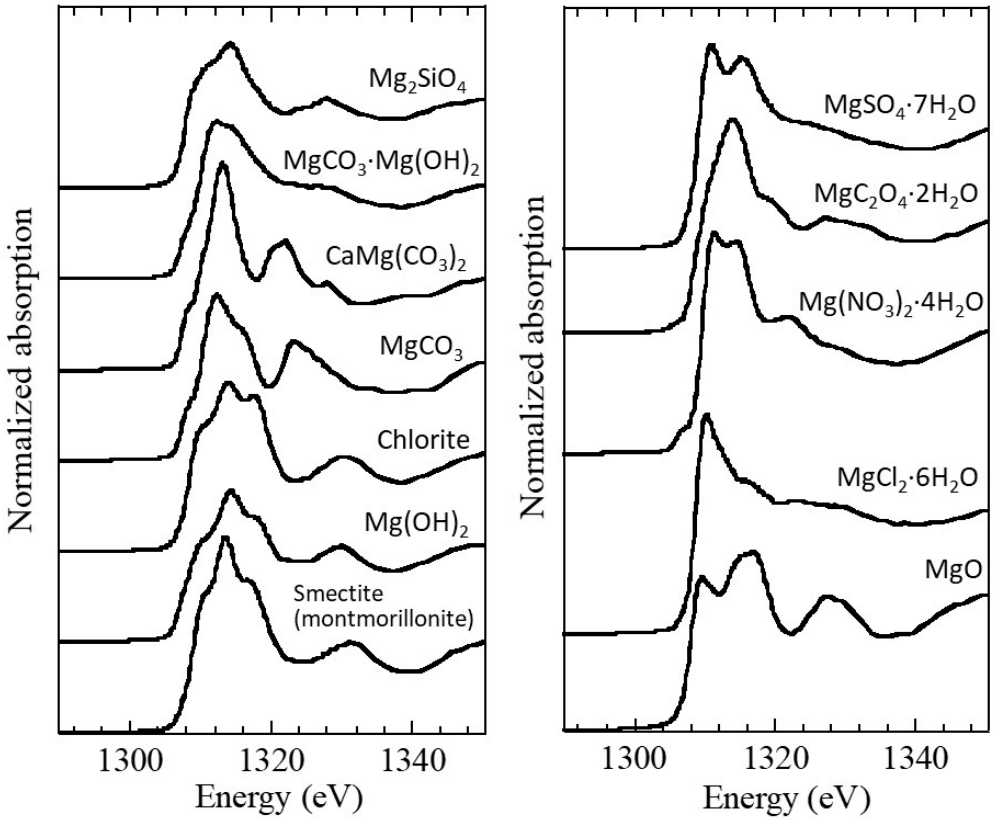

Figure 6. Mg K-edge XANES spectra of (**a**) Mg in natural minerals and (**b**) Mg in other Mg species.

Using these reference materials, the spectra for Mg in aerosol (Figure 7c) were analyzed by LCF based on the spectra of the reference materials in Figure 6. In general, the spectra at any particle size showed the three peaks (or shoulders) specific to octahedral Mg in the phyllosilicates observed in their XANES spectra. This result indicated that the contributions of carbonate and the species that formed secondarily in the atmosphere from carbonate (category (v)) were limited in Mg species in the aerosols. Two examples of the LCF analysis for the speciation of Mg are given for the Stages 1 and 6 samples (Figure 7a,b), considering that the Mg in the finer particles was not important relative to the total Mg in the aerosol samples (<less than 15%). The LCF can reasonably explain the spectra of the aerosol samples, and the Mg species estimated for various particle sizes are shown in Figure 8. As suggested above, the LCF results showed that 71% of Mg was present as octahedral Mg in phyllosilicates, whereas other species, including secondary Mg species (=category (v) defined above) formed in the atmosphere were less than 29% for the total Mg for all particle sizes. The presence of octahedral Mg in phyllosilicates indicated by XANES was consistent with (i) high abundances of illite, chlorite, and montmorillonite (smectite) generally found in aerosols [13,14] and (ii) mineral composition analysis of dust particles in China [15,26] and Japan [24].

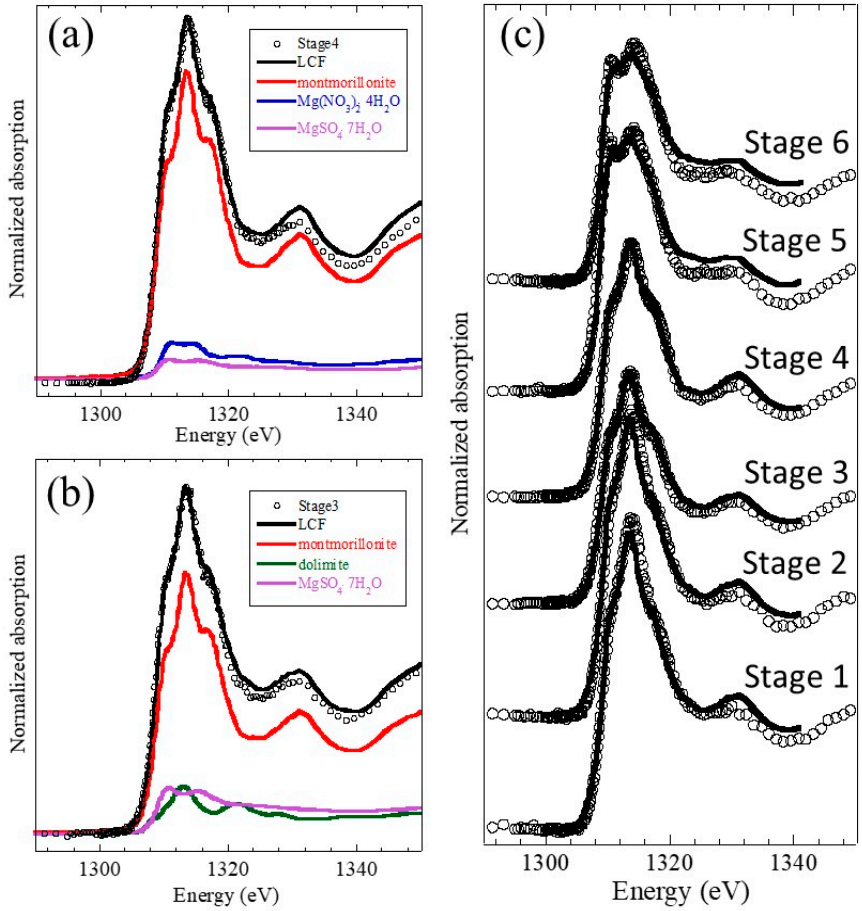

Figure 7. Mg K-edge XANES spectra for Mg in aerosol samples: (**a**) LCF for Mg in (**a**) Stage 4 and (**b**) Stage 3. (**c**) LCF results for XANES spectra of aerosol particles (circle: measured spectra; solid curve: fitted spectra).

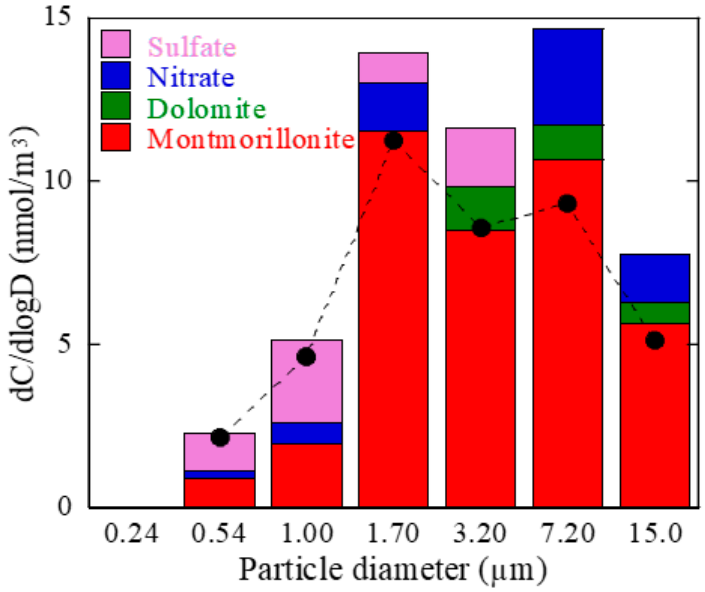

Figure 8. Speciation of Mg in aerosols determined by XANES analyses. Concentration of nss-Mg was also plotted as black circles.

4. Discussion

In Figure 8, [total Mg], including all the Mg species, were plotted as bars. On the other hand, [nss-Mg] was indicated as black circles, which were close to the Mg concentration in Mg-bearing phyllosilicates (=category (i)) for the particle sizes above 1.7 μm. This result clearly showed that [nss-Mg] mainly consisted of Mg-bearing phyllosilicates. This fact also showed that Mg in the aerosols, other than Mg-bearing phyllosilicates, was mainly derived from sea-salt Mg. It is well known that cations in mineral particles react with H_2SO_4 and HNO_3 in the atmosphere, which results in the formation of Mg-sulfate and Mg-nitrate [29,30], shown in Figure 8.

In the finer particles (0.54 and 1.00 μm), [total Mg] was similar to [nss-Mg], whereas the concentration of Mg-bearing phyllosilicates was smaller than [nss-Mg]. This discrepancy suggests that Mg leached from Mg-bearing phyllosilicates forms Mg sulfate through reaction with H_2SO_4 in the atmosphere. In particular, it is known that Mg in the brucite layer in chlorite is reactive, which can be readily leached into water, as suggested in experimental studies [31,32] and natural observations [24]. The fact that the reaction is more active in the finer fractions is consistent with the larger surface area for the finer aerosol samples [2,24].

Most of the Mg-bearing phyllosilicates found in aerosols are (i) illite (typical chemical formula: $(K_{0.75})(Mg_{0.25}Fe_{0.25}Al_{1.5})(Al_{3.5},Si_{0.5})O_{10}(OH)_2$) [28], molar ([Mg]/[Al]) ratio = 0.05), (ii) chlorite ($(Mg_2Al(OH)_6)(Mg_3)(AlSi_3)O_{10}(OH)_2$) [28], molar ([Mg]/[Al]) ratio = 2.5), and (iii) montmorillonite ($(Na_{0.35}Ca_{0.175})(Mg_{0.35}Al_{1.67})(Si_4)O_{10}(OH)_2$) [28], molar ([Mg]/[Al]) ratio = 0.21). The EF(Mg) = 1 for nss-Mg suggests that the molar [Mg]/[Al] ratio for the nss-Mg, consisting mainly of Mg-bearing phyllosilicates, is similar to that of crustal abundance with molar [Mg]/[Al] ratio = 0.31 [23]. This value is within the range from 0.05 to 2.5 for the Mg-bearing phyllosilicates suggested above, supporting the validity of the Mg speciation results.

The LCF also suggested the presence of small amounts of dolomite in the coarser particles, which is also consistent with the presence of $CaCO_3$ in the Ca speciation. The dolomite can be transported directly from the continent because dolomite can be found in desert sand, the loss plateau, and dust collected in East China [15,26]. It is also possible that dolomite can be formed during the evaporation of sea salt droplets in the atmosphere [33]. Thus, it is not easy to distinguish the source of dolomite as a Mg mineral that can neutralize acidic species. It is clear that the contribution of dolomite, or Mg carbonate, to the neutralization of acidic species can be significantly smaller than that of Ca because most of the Mg species in the aerosols are Mg-bearing phyllosilicates.

In the Ca speciation analysis, major species were $CaCO_3$ and its neutralized products. As for Mg speciation, however, not much Mg carbonate (dolomite or magnesite) or its neutralized species were found in the aerosols, but most Mg was mainly present as Mg in phyllosilicates. These results are different from the common assumption in previous studies that most of the Mg species in aerosols are present as carbonate species [5,8,11]. Even if we assume that all of the Mg salts such as Mg sulfate and nitrate were neutralized species formed by the reaction of acidic species and mineral dust, the total amount of reacted Mg shown in Figure 8 is less than 16% of secondary Ca species. Thus, it must be noted that the contribution of Mg in aerosols to the neutralization of acidic species and to buffering the acidity of aerosols is smaller than that assumed in previous studies without precise speciation of Mg in aerosols.

5. Conclusions

In the present study, we applied Mg K-edge XANES for the first time to identification of Mg species in aerosol samples, which revealed that more than 70% of Mg in the aerosols was Mg-bearing phyllosilicates. Since phyllosilicates are much less reactive compared with carbonate, the role of Mg species in neutralization reactions with acidic species (SO_2/H_2SO_4 and HNO_3) and its buffering effect on the acidity of aerosols is not large compared with Ca, mainly present as carbonate in aerosols.

Author Contributions: Conceptualization, Y.T.; methodology, Y.T.; software, Y.Y.; validation, T.K., Y.T., and Y.Y.; formal analysis, T.K.; writing—review and editing, Y.T.; project administration, Y.T.; funding acquisition, Y.T. All authors have read and agreed to the published version of the manuscript.

Funding: This research was funded by Grant-in-Aid for Scientific Research from the Japan Society for Promotion of Science (nos. 19H01960, 19K21893, 18H04134, 17F17332, and 17H06458).

Acknowledgments: XANES analysis was conducted at the SR Center of Ritsumeikan University under the 'Project for Creation of Research Platforms and Sharing of Advanced Research Infrastructure' (proposal Nos.: R1429, R1436, R1469, R1512, R1520, R1565, and R1566). A part of the XANES analysis during this study was also done at SPring-8 (proposal Nos.: 2016A0126, 2016B0126, 2017A0126, and 2017B0126).

Conflicts of Interest: The authors declare no conflict of interest.

References

1. Takahashi, Y.; Miyoshi, T.; Yabuki, S.; Inada, Y.; Shimizu, H. Observation of transformation of calcite to gypsum in mineral aerosols by CaK-edge X-ray absorption near-edge structure (XANES). *Atmos. Environ.* **2008**, *42*, 6535–6541. [CrossRef]
2. Takahashi, Y.; Miyoshi, T.; Higashi, M.; Kamioka, H.; Kanai, Y. Neutralization of Calcite in Mineral Aerosols by Acidic Sulfur Species Collected in China and Japan Studied by Ca K-edge X-ray Absorption Near-Edge Structure. *Environ. Sci. Technol.* **2009**, *43*, 6535–6540. [CrossRef]
3. Seinfeld, J.H.; Pandis, S.N. *Atmospheric Chemistry and Physics: From Air Pollution to Climate Change*; Wiley: Hoboken, NJ, USA, 2012; ISBN 1118591364.
4. Dentener, F.J.; Carmichael, G.R.; Lelieveld, J.; Crutzen, P.J. Role of mineral aerosol as a reactive surface in the global troposhere. *J. Geophys. Res.* **1996**, *101*, 22869–22889. [CrossRef]
5. Maxwell-Meier, K.; Weber, R.; Song, C.; Orsini, D.; Ma, Y.; Carmichael, G.R.; Streets, D.G. Inorganic composition of fine particles in mixed mineral dust-pollution plumes observed from airborne measurements during ACE-Asia. *J. Geophys. Res. D Atmos.* **2004**, *109*, 1–20. [CrossRef]
6. Furukawa, T.; Takahashi, Y. Oxalate metal complexes in aerosol particles: Implications for the hygroscopicity of oxalate-containing particles. *Atmos. Chem. Phys.* **2011**, *11*, 4289–4301. [CrossRef]
7. Miyamoto, C.; Sakata, K.; Yamakawa, Y.; Takahashi, Y. Determination of calcium and sulfate species in aerosols associated with the conversion of its species through reaction processes in the atmosphere and its influence on cloud condensation nuclei activation. *Atmos. Environ.* **2020**, *223*. [CrossRef]
8. Jacobson, M.Z. Studying the effects of calcium and magnesium on size-distributed nitrate and ammonium with EQUISOLV II. *Atmos. Environ.* **1999**, *33*, 3635–3649. [CrossRef]
9. Johnson, M.S.; Meskhidze, N. Atmospheric dissolved iron deposition to the global oceans: Effects of oxalate-promoted Fe dissolution, photochemical redox cycling, and dust mineralogy. *Geosci. Model Dev.* **2013**, *6*, 1137–1155. [CrossRef]
10. Ito, A.; Shi, Z. Delivery of anthropogenic bioavailable iron from mineral dust and combustion aerosols to the ocean. *Atmos. Chem. Phys.* **2016**, *16*, 85–99. [CrossRef]
11. Myriokefalitakis, S.; Daskalakis, N.; Mihalopoulos, N.; Baker, A.R.; Nenes, A.; Kanakidou, M. Changes in dissolved iron deposition to the oceans driven by human activity: A 3-D global modelling study. *Biogeosciences* **2015**, *12*, 3973–3992. [CrossRef]
12. Anthony, J.W.; Bideaux, R.A.; Bladh, K.W.; Nichols, M.C. *Handbook of Mineralogy*; Mineralogical Society of America: Chantilly, VA, USA, 2001.
13. Journet, E.; Balkanski, Y.; Harrison, S.P. A new data set of soil mineralogy for dust-cycle modeling. *Atmos. Chem. Phys.* **2014**, *14*, 3801–3816. [CrossRef]
14. Nickovic, S.; Vukovic, A.; Vujadinovic, M.; Djurdjevic, V.; Pejanovic, G. Technical Note: High-resolution mineralogical database of dust-productive soils for atmospheric dust modeling. *Atmos. Chem. Phys.* **2012**, *12*, 845–855. [CrossRef]
15. Pye, K. *Aeolian Dust and Dust Deposits*; Academic Press: San Diego, CA, USA, 1987.
16. Takahashi, Y.; Kanai, Y.; Kamioka, H.; Ohta, A.; Maruyama, H.; Song, Z.; Shimizu, H. Speciation of sulfate in size-fractionated aerosol particles using sulfur K-edge X-ray absorption near-edge structure. *Environ. Sci. Technol.* **2006**, *40*, 5052–5057. [CrossRef]
17. Sakata, K.; Sakaguchi, A.; Yokoyama, Y.; Terada, Y.; Takahashi, Y. Lead speciation studies on coarse and fine aerosol particles by bulk and micro X-ray absorption fine structure spectroscopy. *Geochem. J.* **2017**, *51*, 215–225. [CrossRef]
18. Kurisu, M.; Adachi, K.; Sakata, K.; Takahashi, Y. Stable Isotope Ratios of Combustion Iron Produced by Evaporation in a Steel Plant. *ACS Earth Sp. Chem.* **2019**, *3*, 588–598. [CrossRef]
19. Draxler, R.R.; Hess, G.D. Description of the HYSPLIT_4 Modeling System. In *NOAA Technical Memorandum ERL ARL-224*; NOAA Air Resource Laboratory: Silver Spring, MD, USA, 2004.
20. Kurisu, M.; Takahashi, Y.; Iizuka, T.; Uematsu, M. Very low isotope ratio of iron in fine aerosols related to its contribution to the surface ocean. *J. Geophys. Res. Atmos.* **2016**, *121*, 11119–11136. [CrossRef]

21. Kelly, S.D.; Hesterberg, D.; Ravel, B. Analysis of Soils and Minerals using X-ray Absorption Spectroscopy. In *Methods of Soil Analysis Part 5—Mineralogical Methods*; Drees, L.R., Uler, A.K., Eds.; Soil Science Society of America Book Series: Madison, WI, USA, 2008; No. 5.
22. Piel, C.; Weller, R.; Huke, M.; Wagenbach, D. Atmospheric methane sulfonate and non-sea-salt sulfate records at the European Project for Ice Coring in Antartica (EPICA) deep-drilling site in Dronning Maud Land, Antarctica. *J. Geophys. Res. Atmos.* **2006**, *111*, 1–13. [CrossRef]
23. Taylor, S.R.; Mclennan, S.M. The geochemical the continental evolution crust. *Rev. Geopysics* **1995**, *33*, 241–265. [CrossRef]
24. Takahashi, Y.; Higashi, M.; Furukawa, T.; Mitsunobu, S. Change of iron species and iron solubility in Asian dust during the long-range transport from western China to Japan. *Atmos. Chem. Phys.* **2011**, *11*, 11237–11252. [CrossRef]
25. Zhou, G.; Tazaki, K. Seasonal variation of gypsum in aerosol and its effect on the acidity of wet precipitation on the Japan Sea side of Japan. *Atmos. Environ.* **1996**, *30*, 3301–3308. [CrossRef]
26. Wei, L.; Qi, F.; Tao, W.; Yanwu, Z.; Jianhua, S. Physicochemistry and mineralogy of storm dust and dust sediment in northern China. *Adv. Atmos. Sci.* **2004**, *21*, 775–783. [CrossRef]
27. Vespa, M.; Dähn, R.; Huthwelker, T.; Wieland, E. Soft X-ray absorption near-edge investigations of Mg-containing mineral phases relevant for cementitious materials. *Phys. Chem. Earth* **2017**, *99*, 168–174. [CrossRef]
28. Langmuir, D. *Aqueous Environmental Geochemistry*; Prentice Hall: Hoboken, NJ, USA, 1997.
29. Ha, Z.; Chan, C.K. The Water Activities of $MgCl_2$, $Mg(NO_3)_2$, $MgSO_4$, and Their Mixtures. *Aerosol Sci. Technol.* **1999**, *31*, 154–169. [CrossRef]
30. Wang, J.; Morin, C.; Li, L.; Hitchcock, A.P.; Scholl, A.; Doran, A. Radiation damage in soft X-ray microscopy. *J. Electron. Spectros. Relat. Phenom.* **2009**, *170*, 25–36. [CrossRef]
31. Zänker, H.; Hüttig, G.; Arnold, T.; Nitsche, H. Formation of iron-containing colloids by the weatheringof phyllite. *Aquat. Geochem.* **2006**, *12*, 299–325. [CrossRef]
32. Brandt, F.; Bosbach, D.; Krawczyk-Barsch, E.; Arnold, T.; Bernhard, G. Chlorite dissolution in the acid ph-range: A combined microscopic and macroscopic approach. *Geochim. Cosmochim. Acta* **2003**, *67*, 1451–1461. [CrossRef]
33. Bochert, H. *Chemical Oceanography*; Academic Press: London, UK, 1965.